Space Weather

RESEARCH ARTICLE
10.1029/2023SW003477

# Enhanced Radiation Levels at Aviation Altitudes and Their Relationship to Plasma Waves in the Inner Magnetosphere

**Homayon Aryan[1], Jacob Bortnik[1], W. Kent Tobiska[2], Piyush Mehta[3], and Rashmi Siddalingappa[3]**

[1]Atmospheric and Oceanic Sciences, University of California Los Angeles, Los Angeles, CA, USA, [2]Space Weather Division, Space Environment Technologies, Pacific Palisades, CA, USA, [3]Mechanical and Aerospace Engineering, West Virginia University, Morgantown, WV, USA

**Key Points:**

- We report on observation of enhanced radiation levels at aviation altitudes and their relationship to various plasma waves
- We study the Automated Radiation Measurements for Aerospace Safety (ARMAS) conjunctions with the Van Allen Probes
- Dose rate observed by ARMAS at aviation altitudes is only correlated to plasmaspheric hiss waves observed in the inner magnetosphere

**Correspondence to:**
H. Aryan,
aryan.homayon@gmail.com

**Citation:**
Aryan, H., Bortnik, J., Tobiska, W. K., Mehta, P., & Siddalingappa, R. (2023). Enhanced radiation levels at aviation altitudes and their relationship to plasma waves in the inner magnetosphere. *Space Weather*, *21*, e2023SW003477. https://doi.org/10.1029/2023SW003477

Received 5 MAR 2023
Accepted 5 JUN 2023



**Abstract** It is believed that galactic cosmic rays and solar energetic particles are the two major sources of ionizing radiation. However, the radiation source may also be due to relativistic electrons that are associated with precipitation from the Van Allen radiation belts. In this study, we use Automated Radiation Measurements for Aerospace Safety (ARMAS) measurements to investigate the precipitation mechanism of energetic radiation belt electrons. ARMAS instruments are flown on agency-sponsored (NASA, National Oceanic and Atmospheric Administration, National Science Foundation, Federal Aviation Administration, DOE) flights, commercial space transportation companies and airliners (>9 km) in automated radiation collection mode. We identified magnetic conjunction events between ARMAS and NASA's Van Allen Probes to study the highly variable, dynamic mesoscale radiation events observed by ARMAS instruments at aviation altitudes and their relationship to various plasma waves in the inner magnetosphere measured by the Van Allen Probes. The results show that there is a strong correlation between dose rates observed by ARMAS and plasmaspheric hiss wave power measured by the Van Allen Probes, but no such relationship with electromagnetic ion cyclotron waves and only a modest correlation with whistler mode chorus waves. These results suggest that the space environment could have a potentially significant effect on passenger safety.

## 1. Introduction

For many decades it was believed that the galactic cosmic rays (GCRs) and solar energetic particles (SEPs) are the two major sources of radiation hazards (Reames, 2013; Vlahos et al., 2019). GCRs consist mostly of energetic protons, and may also contain heavy ions such as iron, that are produced in high-energy explosive events outside the solar system and modulated slowly by the interplanetary magnetic field (IMF) (Blandford & Eichler, 1987). SEPs originate from flaring events related to solar coronal mass ejections (CMEs) on the Sun or from IMF shocks (Desai & Giacalone, 2016; Gopalswamy et al., 2004; Reames, 2013). However, recently it has been shown that the radiation source may also be due to relativistic electrons that are precipitated from the Van Allen radiation belts (Tobiska et al., 2018) and may be related to electromagnetic ion cyclotron (EMIC) waves (Tobiska et al., 2022). The latter study has used the flight measurements by the Automated Radiation Measurements for Aerospace Safety (ARMAS) experiment to uncover the potential source for aviation radiation as relativistic electron precipitation from the Van Allen radiation belts. Energetic radiation belt electrons precipitate into the Earth's atmosphere and can pose serious hazard to pilots, aircraft passengers, and commercial space travelers (Bennett et al., 2013; Kataoka et al., 2015; Knipp, 2017). In this study we use the ARMAS measurements to understand the precipitation mechanism of energetic radiation belt electrons and their relationship to various plasma waves in the inner magnetosphere measured by the Van Allen Probes.

The charged particles enter the Earth's atmosphere at different magnetic latitudes and impact atmospheric molecules. Cosmic radiation exposure directly impacts human health by increasing the risk of fatal cancer or other adverse health effects to air travelers (Knipp, 2017). Cosmic radiation has also been linked to space weather affects such as Single Event Effects (SEEs) (e.g., Gatsonis 1997; Olsen et al., 1993). We identified conjunction events between ARMAS observations on commercial altitude (>9 km) aircraft and NASA's Van Allen Probes in terms of Magnetic Local Time (MLT) and L-Shell (L). We then identified significantly enhanced radiation events to study the highly variable, dynamic mesoscale radiation events observed by ARMAS at aviation altitudes and their relationship to various plasma waves, measured by the Van Allen Probes, in the inner magnetosphere.

## 2. Data and Methodology

The ARMAS instruments are flown in an automated radiation collection mode on agency-sponsored flights such as, the National Oceanic and Atmospheric Administration (NOAA), the National Science Foundation (NSF), the National Center for Atmospheric Research (NCAR), the NASA Armstrong Flight Research Center (AFRC), the Federal Aviation Administration (FAA) William J. Hughes Technical Center (WJHTC) Bombardier Global 5000 (BG5), Gulfstream 5 (G-5), and commercial aircrafts (Tobiska et al., 2016, 2018, 2022). The ARMAS monitoring system consists of two components: (a) a flight instrument that measures the environment absorbed dose in silicon on an aircraft and (b) a real-time data stream from the aircraft to the ground (Tobiska et al., 2016, 2018, 2022). The data is then processed to Level 4 effective dose rates for location and time. The absorbed dose (Si) is measured within the aircraft, it is relayed to the ground via an Iridium satellite link or aircraft WiFi. The measurements are made using the Teledyne micro dosimeter uDOS001 (uDOS) in combination with a microprocessor, a GPS chip, an Iridium transceiver or a Bluetooth transmitter, and associated electronics. The uDOS chip is sensitive to heavy ions (Fe+), alphas, protons, neutrons, electrons, and $\gamma$-rays, especially above 1 MeV based on extensive ground beam line testing (Tobiska et al., 2016). In this study, we use almost 7 years of ARMAS real-time radiation measurements (2013–2019) from ground to 107 km altitude for >700 flights consisting >700,000 10-s measured absorbed dose and derived effective dose rates. The background dose, in this study, are estimated by NASA Langley Research Center (LaRC) Nowcast of Atmospheric Ionizing Radiation for Aviation Safety (NAIRAS) model (Mertens et al., 2013), which includes GCR. The background will also include SEPs.

The Van Allen Probes were launched on 30 August 2012 and were operational until 2019. The two identical probes were launched into a 10° inclination orbit with a perigee of approximately 1.1 RE and an apogee of 5.8 RE geocentric (Mauk et al., 2013). Each probe carried an Electric and Magnetic Field Instrument Suite and Integrated Science (EMFISIS) wave instrument to measure wave power spectral density (PSD) between 10 Hz and 12 kHz using a Waveform Receiver (Kletzing et al., 2013; Wygant et al., 2013) and the high-frequency receiver (HFR) that measured electric spectral intensity between 10 and 400 kHz. The background magnetic fields were measured via a triaxial fluxgate magnetometer while the high frequency wave magnetic field fluctuations were measured by a triaxial search coil magnetometer (Kletzing et al., 2013). The EMFISIS waves instruments provided a comprehensive set of electric and magnetic field wave measurements needed to identify various wave types within the inner magnetosphere. We use the comprehensive wave data measurements from the EMFISIS instruments, for the entire Van Allen Probes mission, to identify different types of waves and study the relationship between each wave type with enhanced radiation events measured by ARMAS during conjunction events with each Van Allen Probe. The 3D magnetic field waveforms, which were captured in a continuous waveform burst mode with selected ~6 s snapshots from search coil magnetometers, are used to calculate the wave intensities and the HFR are used to calculate the high frequency wave intensities.

For EMIC waves, the magnetic field intensities, Bw, are calculated by integrating the wave spectral intensities ($pT^2\ Hz^{-1}$) over the frequency ranges $f_{cHe^+} < f < f_{cH^+}$, $f_{cO^+} < f < f_{cHe^+}$, and $f < f_{cO^+}$ for $H^+$, $He^+$, and $O^+$ bands respectively (Usanova et al., 2012; Yu et al., 2021). The magnetic field intensities, Bw, for high frequency waves are calculated by integrating the wave spectral intensities ($pT^2\ Hz^{-1}$) over the frequency range $f > f_{ce}$. For plasmaspheric hiss, the magnetic field intensities, Bw, are calculated by integrating the wave spectral intensities ($pT^2\ Hz^{-1}$) over the frequency range 100 Hz < f < 2 kHz (Aryan et al., 2016; Meredith et al., 2004, 2007; Thorne et al., 1973). Whilst the magnetic field intensities for whistler mode chorus waves are calculated by integrating the wave spectral intensities ($pT^2\ Hz^{-1}$) over the frequency range $0.1f_{ce} < f < 0.5f_{ce}$ (Aryan et al., 2014, 2016; Meredith et al., 2001, 2012). Chorus and plasmaspheric hiss waves are distinguished by the plasma density where frequencies overlap (for more details please see Aryan et al. (2014, 2016, 2022), and Sheeley et al. (2001)).

Figure 1 shows a schematic of the Van Allen Probes observing plasma waves in the inner magnetosphere while in magnetic conjunction with ARMAS instrument at aviation altitudes (top panel). The middle panel shows the background dose rate (black line) and the observed dose rate (red bars) measured by ARMAS instruments. Plasma wave observations by the Van Allen Probes are shown in the bottom panel. In this particular example, the Van Allen Probe B observed plasmaspheric hiss waves while in magnetic conjunction with ARMAS on 29 March 2018. The solid and dotted blue lines represent the difference in L-Shell (ΔL (RE)) and MLT (ΔMLT (h)) respectively between ARMAS and Van Allen Probe B. At the same time ARMAS also observed dose rates much higher than the background dose rate. The two observations coincide well, as the highest dose rate was observed when the most intense plasmaspheric hiss wave power was recorded by Van Allen Probe B between 19:36UT to

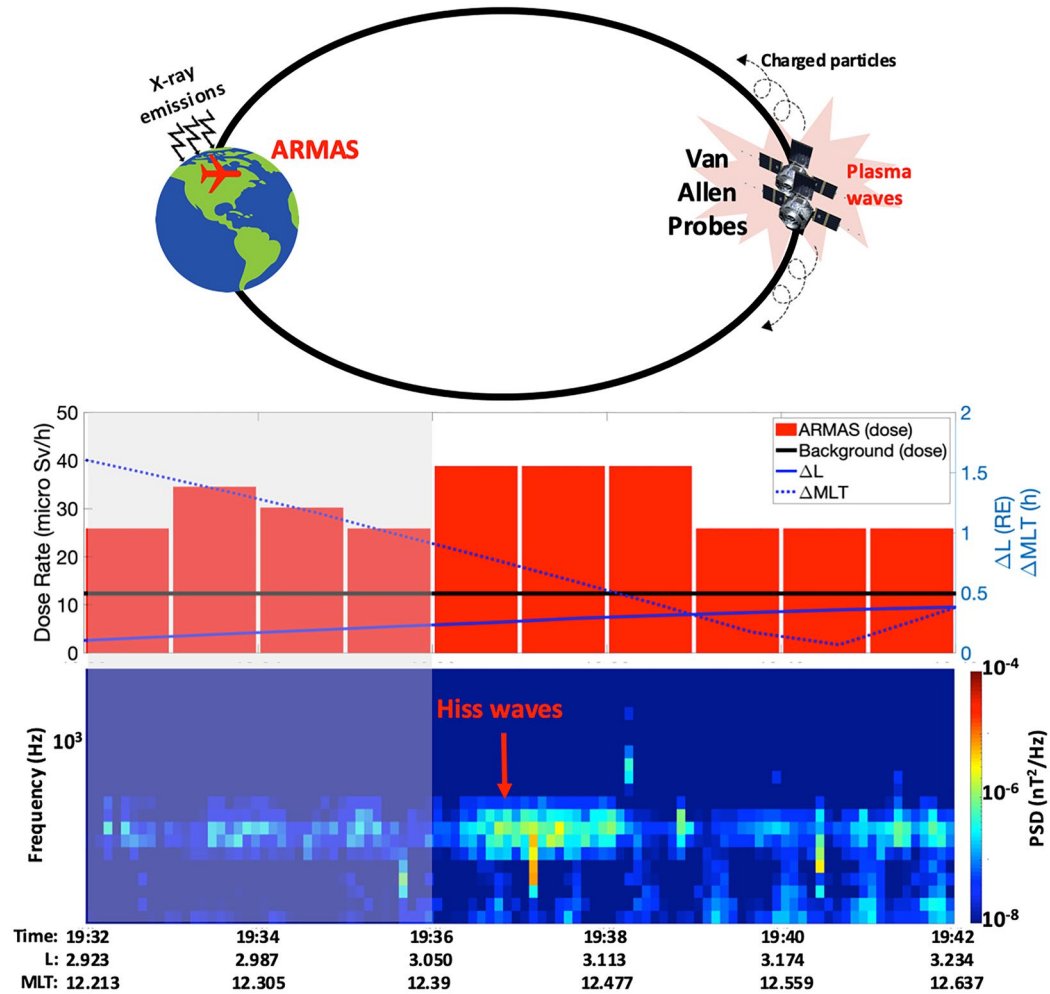


**Figure 1.** A schematic of the Van Allen Probes observing plasma waves in the inner magnetosphere while in magnetic conjunction with Automated Radiation Measurements for Aerospace Safety (ARMAS) instrument at aviation altitudes (top panel). The middle panel shows the background dose rate (black line) and the observed dose rate (red bars) measured by ARMAS. Plasma wave observations by the Van Allen Probes are shown in the bottom panel. In this particular example the Van Allen Probe B is observing plasmaspheric hiss waves while in magnetic conjunction with ARMAS on 29 March 2018. The solid and dotted blue lines in the middle panel shows ΔL and ΔMLT respectively between ARMAS and Van Allen Probe B

19:39UT during the closest conjunction period (between 19:36UT to 19:42UT) with both ΔL and ΔMLT less than 1 (the gray shaded area highlights times when ARMAS and Van Allen Probe B is not in close conjunction i.e., ΔL or/and ΔMLT is greater than 1).

## 3. Results and Discussions

### 3.1. ARMAS Conjunctions With the Van Allen Probes

We identified conjunction events between ARMAS and the Van Allen Probes for enhanced radiation events observed by ARMAS at aviation altitudes. Figure 2 shows the number of conjunctions between ARMAS and the Van Allen Probes as a function of ΔL and ΔMLT. The number of conjunctions increases with increasing ΔL and ΔMLT. The aim is to keep the conjunction window, in terms of time (ΔMLT) and space (ΔL), as small as possible to ensure the observations between ARMAS and the Van Allen Probes are related, whilst ensuring there are reasonable number of data (conjunctions) to study the relationship between enhanced radiation events at aviation altitudes (>9 km) and various plasma waves in the inner magnetosphere. The results, presented in Figure 2, shows that there are more than 1,000 conjunction points for a conjunction window of ΔL < 1RE and

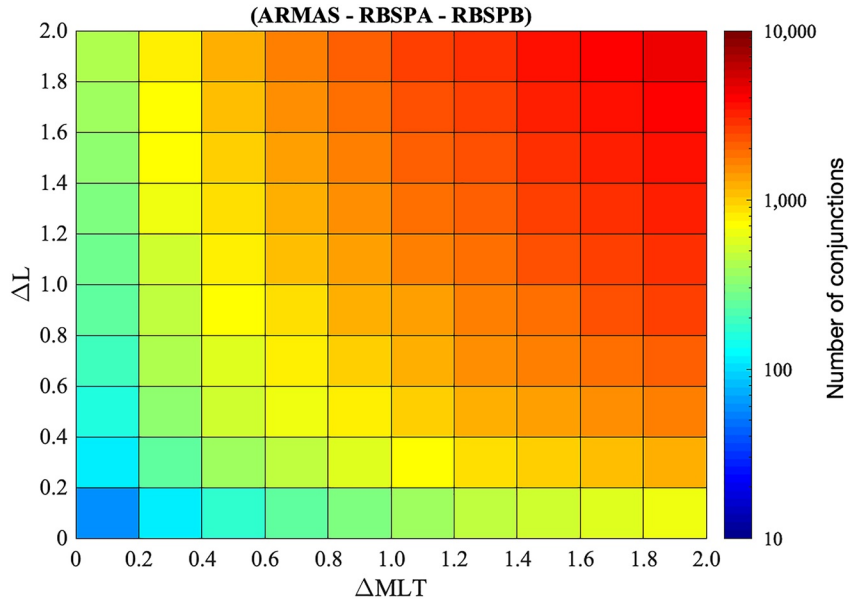


**Figure 2.** The conjunctions events between Automated Radiation Measurements for Aerospace Safety (ARMAS) and the Van Allen Probes. The number of conjunctions between ARMAS and the Van Allen Probes are shown as a function of ΔL and ΔMLT.

ΔMLT < 1 hr, which is a reasonable size, and enough to conduct the statistical study (please note that 1RE is considerably larger than the scale of the waves discussed here; Aryan et al., 2021, 2022; Blum et al., 2017; Zhang et al., 2021).

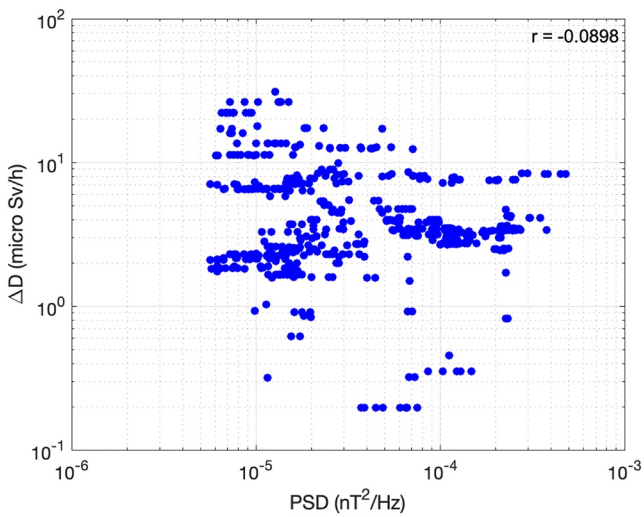


**Figure 3.** The correlation between the dose rate observed by Automated Radiation Measurements for Aerospace Safety at aviation altitudes and wave power in the electromagnetic ion cyclotron frequency range observed by the Van Allen Probes in the inner magnetosphere. The correlation coefficient is given in the top right.

### 3.2. Correlation Between Enhanced Radiation at Aviation Altitude and EMIC Waves

It has been suggested, in the past, that the third source of enhanced radiation observed at aviation altitude might be related to the occurrence of EMIC waves in the inner magnetosphere (Tobiska et al., 2022; Tsurutani et al., 2016). EMIC waves are generally excited by anisotropic protons in the ring current when heavy ions, such as He+ and O+ are present within the background plasma. They are often observed within three distinct bands (the H+ band, He+ band, and O+ band) in the terrestrial magnetosphere and due to the presence of He+, O+, and H+ in the background plasma, new resonances arise at the gyrofrequencies of He+ and O+ (Allen et al., 2015; Min et al., 2012; Saikin et al., 2015; Yu et al., 2015). In this section we study statistically the correlation between the ARMAS observed dose rate and wave power in the EMIC frequency range. Figure 3 shows the relationship between dose rate (ΔD) observed by ARMAS and wave PSD observed by the Van Allen Probes during conjunction events, over the frequency ranges $f_{cHe^+} < f < f_{cH^+}$, $f_{cO^+} < f < f_{cHe^+}$, and $f < f_{cO^+}$ for $H^+$, $He^+$, and $O^+$ bands respectively (Note: ΔD is the difference between the measured dose by ARMAS and the background dose estimated by NAIRAS model. Also each point represents 1 min of measurement and the EMIC wave intensity is the sum of the intensities of the three bands). The results show that there is no correlation between enhanced radiation and wave power in the EMIC frequency range with the correlation coefficient of $r = -0.0898$. This indicates that the source might be related to a different type of plasma that influences the dynamics of the radiation belts.

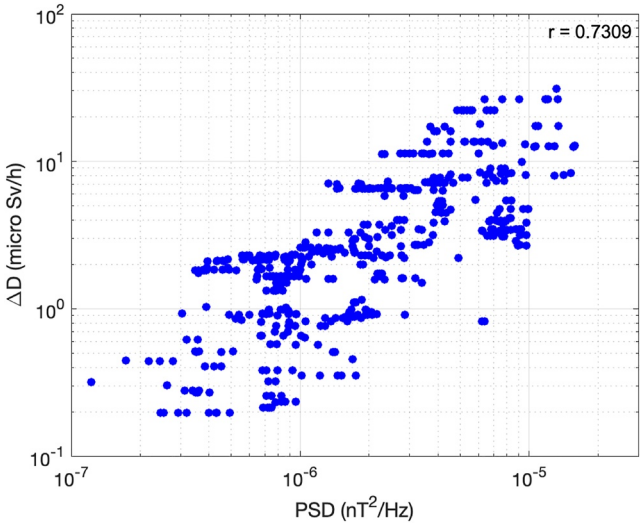


**Figure 4.** The correlation between the dose rate observed by Automated Radiation Measurements for Aerospace Safety at aviation altitudes and plasmaspheric hiss wave power observed by the Van Allen Probes in the inner magnetosphere. The correlation coefficient is given in the top right.

### 3.3. Correlation Between Enhanced Radiation at Aviation Altitude and Plasmaspheric Hiss Waves

Plasmaspheric hiss waves are excited naturally in the high plasma density region inside the plasmasphere and dayside plasmaspheric plumes (Chan & Holzer, 1976; Hayakawa et al., 1986; Parrot & Lefeuvre, 1986) and are known to be largely responsible for the continuous scattering of the inner radiation belt electrons into the atmospheric loss cone, the decay of energetic electrons in the outer radiation belt during relatively quiet geomagnetic conditions (Lyons et al., 1972; Summers et al., 2007) due to resonant pitch angle scattering of energetic electrons (Lyons et al., 1972), and are responsible for the formation of the slot region between the inner and outer radiation belts (Abel & Thorne, 1998; Lyons & Thorne, 1973; Lyons et al., 1972). Plasmaspheric hiss waves are right hand polarized electromagnetic whistler mode wave (Bortnik et al., 2008, 2009; Thorne et al., 1973) observed as a steady, incoherent noise band (Falkowski et al., 2017; Tsurutani et al., 2015, 2018) and typically observed in the frequency range 100 Hz $< f <$ 2 kHz with a lower wave power than chorus (Meredith et al., 2004).

Figure 4 shows the relationship between dose rate (ΔD) observed by ARMAS and plasmaspheric hiss wave PSD observed by the Van Allen Probes during conjunction events. The results show that there is a strong correlation between enhanced radiation levels observed at aviation altitudes and plasmaspheric hiss wave power observed along the same magnetic field line in the plasmasphere with a correlation coefficient of $r = 0.7309$. This indicates that the radiation source at aviation altitudes may also be due to the continuous scattering of radiation belt electrons by plasmaspheric hiss waves.

### 3.4. Correlation Between Enhanced Radiation at Aviation Altitude and Chorus Waves

Chorus waves are excited by the injection of substorm electrons in the vicinity of the geomagnetic equator (Burtis & Helliwell, 1969; Lauben et al., 2002; LeDocq et al., 1998; Meredith et al., 2001; Tsurutani & Smith, 1974) associated with the electron temperature anisotropy plasma instability (Kennel & Petschek, 1966). Chorus waves are very intense right hand polarized electromagnetic whistler mode waves that make significant contributions to the production of the diffuse aurora (Ni et al., 2008; Thorne, 2010) and are an important source of plasmaspheric hiss waves (Agapitov et al., 2018; Bortnik et al., 2008, 2009, 2016; Meredith et al., 2013). Chorus emissions are observed in the low density region outside the plasmasphere as short coherent pulses (Burtis & Helliwell, 1969; Tsurutani & Smith, 1974) in the frequency range of $0.1f_{ce} < f < f_{ce}$ ($0.1f_{ce} < f < 0.5f_{ce}$ is defined as the lower band chorus and $0.5f_{ce} < f < f_{ce}$ is the upper band chorus), where $f_{ce}$ is the local electron gyrofrequency. The lower band chorus is believed to be the dominant scattering process leading to pulsating auroral precipitation (Nishimura et al., 2010, 2011).

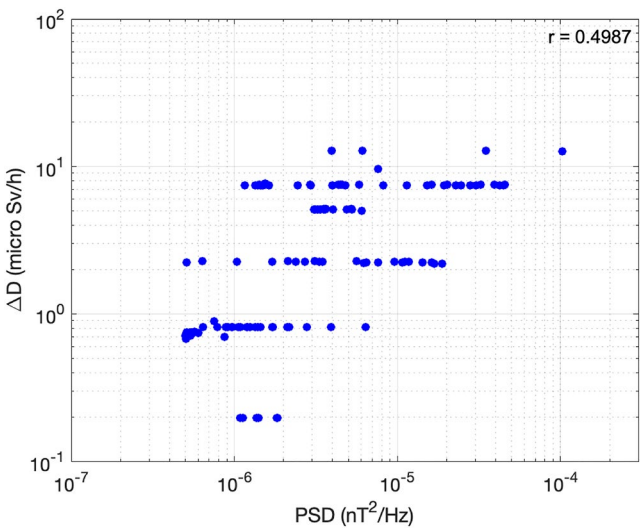


**Figure 5.** The correlation between the dose rate observed by Automated Radiation Measurements for Aerospace Safety at aviation altitudes and chorus wave power observed by the Van Allen Probes in the inner magnetosphere. The correlation coefficient is given in the top right.

Figure 5 shows the relationship between the dose rate (ΔD) observed by ARMAS and chorus wave PSD observed by the Van Allen Probes during conjunction events. The results show that there may be a relationship between enhanced radiation at aviation altitude and chorus wave power in the inner magnetosphere with a correlation coefficient of $r = 0.4987$. Also, there are relatively fewer chorus wave observations during the conjunction events, and therefore the relationship may be better defined with a larger number of chorus wave observations.

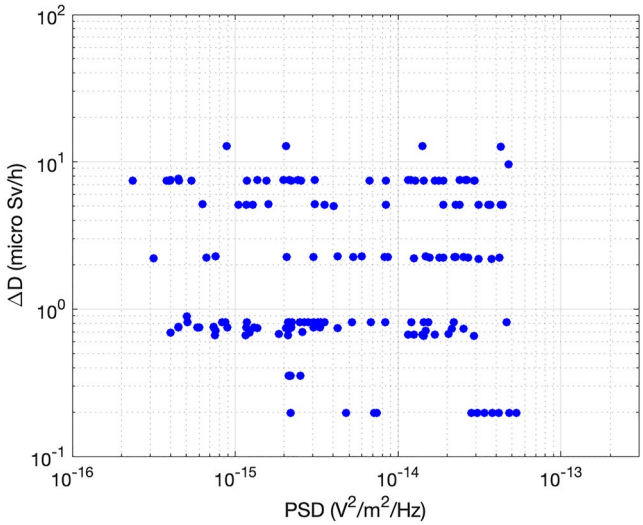


**Figure 6.** The correlation between the dose rate observed by Automated Radiation Measurements for Aerospace Safety at aviation altitudes and wave power in the high frequency range observed by the Van Allen Probes in the inner magnetosphere. The correlation coefficient is given in the top right.

### 3.5. Correlation Between Enhanced Radiation at Aviation Altitude and High Frequency Waves

For completeness we also tested the relationship between enhanced radiation at aviation altitude and wave PSD in the high frequency range (i.e., $f > f_{ce}$) which includes potential scattering from Electrostatic Electron Cyclotron Harmonic (ECH) waves (Fukizawa et al., 2018; Horne et al., 2003; Kennel et al., 1970; Kurita et al., 2014). Figure 6 shows the relationship between dose rate (ΔD) observed by ARMAS and wave PSD in the high frequency range observed by the Van Allen Probes during conjunction events. The results show that there is no correlation between enhanced radiation and high frequency wave power with the correlation coefficient of $r = -0.0252$. This indicates that the source might not be related to any plasma waves above $f_{ce}$, and highlights plasmaspheric hiss as the leading scattering candidate.

### 3.6. Dose Rate Versus Plasmaspheric Hiss Wave Power as a Function of Geomagnetic Activity

In Section 3.3 it was shown that there is a strong correlation between enhanced radiation at aviation altitudes and plasmaspheric hiss wave power in the plasmasphere with a correlation coefficient of $r = 0.7309$. It has been shown that plasmaspheric hiss wave power is determined by the level of geomagnetic activity as defined by geomagnetic index AE (Aryan et al., 2021). In this section we study how the relationship between dose rate and plasmaspheric hiss wave power, shown in Section 3.3, is affected by the level of geomagnetic activity. Figure 7 shows the relationship between dose rate (ΔD) observed by ARMAS and plasmaspheric hiss wave PSD observed by the Van Allen Probes during conjunction events as a function of low (AE < 100 nT), medium (100 nT < AE < 300 nT), and high (AE > 300 nT) geomagnetic activities. The results show that the correlation coefficient between observed dose rate by ARMAS at aviation altitudes and plasmaspheric hiss wave power observed in the inner magnetosphere decreases as geomagnetic activity increases, which may be related. Also, higher geomagnetic activity leads to more intense plasmaspheric hiss wave power that ultimately leads to more enhanced radiation at aviation altitudes at all activity levels.

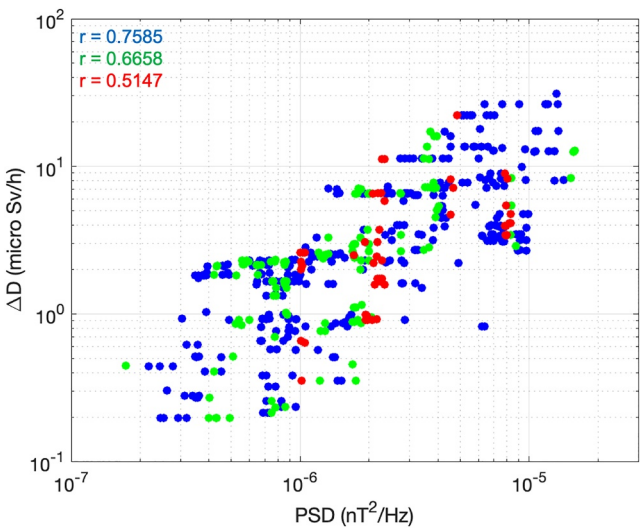


**Figure 7.** The relationship between the dose rate (ΔD) observed by Automated Radiation Measurements for Aerospace Safety and plasmaspheric hiss wave power spectral density observed by the Van Allen Probes during conjunction events as a function of geomagnetic activity. The blue, green, and red stars represents low (AE < 100 nT), medium (100 nT < AE < 300 nT), and high (AE > 300 nT) geomagnetic activities respectively.

### 3.7. Dose Rate Versus Plasmaspheric Hiss Wave Power as a Function of Plasma Density

The plasma density plays an important role in determining the wave propagation characteristics (Bortnik et al., 2008, 2009, 2011; Breneman et al., 2009; Chen et al., 2012; Hartley et al., 2018; Malaspina et al., 2018). Here we show how the relationship between the dose rate observed by ARMAS and the plasmaspheric hiss wave power observed by the Van Allen Probes, as shown in Section 3.3, is affected by plasma density. Figure 8 shows the relationship between dose rate (ΔD) observed by ARMAS and plasmaspheric hiss wave PSD observed by the Van Allen Probes during conjunction events as a function of low ($n_e < 100$ cm$^{-3}$), medium (100 cm$^{-3}$ < $n_e$ < 300 cm$^{-3}$), and high ($n_e > 300$ cm$^{-3}$) plasma densities. The results show that the correlation coefficient between dose rate and plasmaspheric hiss wave power is generally similar for all differ-

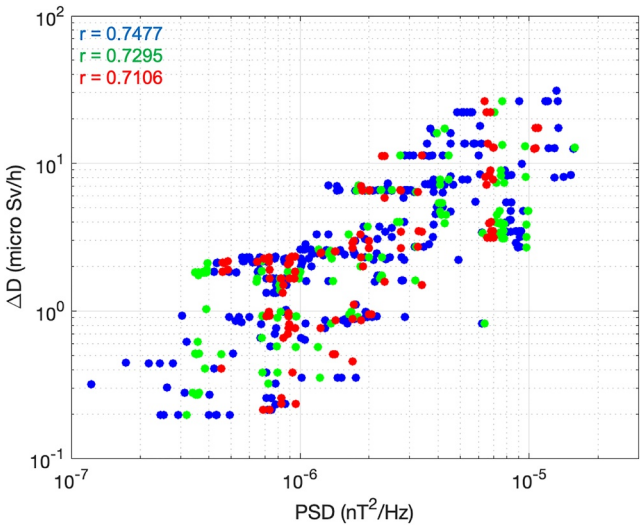


**Figure 8.** The relationship between dose rate (ΔD) observed by Automated Radiation Measurements for Aerospace Safety and plasmaspheric hiss wave power spectral density observed by the Van Allen Probes during conjunction events as a function of plasma density. The blue, green, and red stars represents low ($n_e < 100$ cm$^{-3}$), medium (100 cm$^{-3}$ < $n_e$ < 300 cm$^{-3}$), and high ($n_e > 300$ cm$^{-3}$) plasma densities respectively.

ent densities, although, higher density events are slightly more likely to occur at more intense plasmaspheric hiss wave power.

## 4. Conclusion

In this study, we used almost 7 years of ARMAS real-time radiation measurements taken at aviation altitudes (>9 km) and plasma wave data observed by NASA's Van Allen Probes in the inner magnetosphere (between 2013 and 2019). We identified conjunction events between ARMAS and Van Allen Probes, focusing on enhanced radiation events, and studied the relationship between dose rate and various magnetospheric waves. The results show that there is a strong correlation between the observed dose rate and plasmaspheric hiss wave power. However, there is no correlation between dose rate and other plasma wave types in the inner magnetosphere, such as, EMIC waves, high-frequency waves, and possibly also whistler mode chorus, although the results for chorus waves were somewhat unclear. As we understand the two major sources of ionizing radiation hazards are the GCRs and SEPs. However, the results presented here shows that an additional radiation source is also due to plasmaspheric hiss waves within the inner magnetosphere. The results also show that geomagnetic activity may also play an important role in defining the relationship between enhanced radiation and plasmaspheric hiss waves in the inner magnetosphere. Overall the results suggest that the space environment could have a potentially significant effect to pilots, aircraft passengers, and commercial space travellers.

## Data Availability Statement

The HFR and WFR data are freely available from the EMFISIS instrument (Kletzing et al., 2013; Wygant et al., 2013) website at the University of Iowa (https://emfisis.physics.uiowa.edu/). The geomagnetic index (AE) are freely available from NASA's GSFC online space physics data facility, OMNIWeb (https://omniweb.gsfc.nasa.gov). The ARMAS data is freely available from Space Environment Technologies ARMAS website at https://spacewx.com/radiation-decision-aids/.

**Acknowledgments**
This study is supported by NASA's Living With Start (LWS) program (NASA/LWS-ARMAS: 443956-BR-23267).

## References

Abel, B., & Thorne, R. M. (1998). Electron scattering loss in Earth's inner magnetosphere 1. Dominant physical processes. *Journal of Geophysical Research*, *103*(A2), 2385–2396. https://doi.org/10.1029/97JA02919

Agapitov, O. V., Mourenas, D., Artemyev, A. V., Mozer, F. S., Hospodarsky, G., Bonnell, J., & Krasnoselskikh, V. (2018). Synthetic empirical chorus wave model from combined Van Allen Probes and Cluster statistics. *Journal of Geophysical Research: Space Physics*, *123*(1), 297–314. https://doi.org/10.1002/2017JA024843

Allen, R. C., Zhang, J.-C., Kistler, L. M., Spence, H. E., Lin, R.-L., Klecker, B., et al. (2015). A statistical study of emic waves observed by cluster: 1. Wave properties. *Journal of Geophysical Research: Space Physics*, *120*(7), 5574–5592. https://doi.org/10.1002/2015JA021333

Aryan, H., Bortnik, J., Meredith, N. P., Horne, R. B., Sibeck, D. G., & Balikhin, M. A. (2021). Multi-parameter chorus and plasmaspheric hiss wave models. *Journal of Geophysical Research: Space Physics*, *126*(1), e2020JA028403. https://doi.org/10.1029/2020JA028403

Aryan, H., Bortnik, J., Sibeck, D. G., & Hospodarsky, G. (2022). Global map of chorus wave sizes in the inner magnetosphere. *Journal of Geophysical Research: Space Physics*, *127*(3), e2021JA029768. https://doi.org/10.1029/2021JA029768

Aryan, H., Sibeck, D., Balikhin, M., Agapitov, O., & Kletzing, C. (2016). Observation of chorus waves by the Van Allen Probes: Dependence on solar wind parameters and scale size. *Journal of Geophysical Research (Space Physics)*, *121*(8), 7608–7621. https://doi.org/10.1002/2016JA022775

Aryan, H., Yearby, K., Balikhin, M., Agapitov, O., Krasnoselskikh, V., & Boynton, R. (2014). Statistical study of chorus wave distributions in the inner magnetosphere using ae and solar wind parameters. *Journal of Geophysical Research (Space Physics)*, *119*(8), 6131–6144. https://doi.org/10.1002/2014JA019939

Bennett, L., Lewis, B., Bennett, B., McCall, M., Bean, M., Doré, L., & Getley, I. (2013). A survey of the cosmic radiation exposure of air Canada pilots during maximum galactic radiation conditions in 2009. *Radiation Measurements*, *49*, 103–108. https://doi.org/10.1016/j.radmeas.2012.12.004

Blandford, R., & Eichler, D. (1987). Particle acceleration at astrophysical shocks: A theory of cosmic ray origin. *Physics Reports*, *154*(1), 1–75. https://doi.org/10.1016/0370-1573(87)90134-7

Blum, L. W., Bonnell, J. W., Agapitov, O., Paulson, K., & Kletzing, C. (2017). Emic wave scale size in the inner magnetosphere: Observations from the dual Van Allen Probes. *Geophysical Research Letters*, *44*(3), 1227–1233. https://doi.org/10.1002/2016GL072316

Bortnik, J., Chen, L., Li, W., Thorne, R. M., & Horne, R. B. (2011). Modeling the evolution of chorus waves into plasmaspheric hiss. *Journal of Geophysical Research*, *116*(A8), A08221. https://doi.org/10.1029/2011JA016499

Bortnik, J., Chen, L., Li, W., Thorne, R. M., Nishimura, Y., Angelopoulos, V., & Kletzing, C. A. (2016). *Relationship between chorus and plasmaspheric hiss waves* (Vol. 216, pp. 79–97). Washington DC American Geophysical Union Geophysical Monograph Series. https://doi.org/10.1002/9781119055006.ch6

Bortnik, J., Li, W., Thorne, R. M., Angelopoulos, V., Cully, C., Bonnell, J., et al. (2009). An observation linking the origin of plasmaspheric hiss to discrete chorus emissions. *Science*, *324*(5928), 775–778. https://doi.org/10.1126/science.1171273

Bortnik, J., Thorne, R. M., & Meredith, N. P. (2008). The unexpected origin of plasmaspheric hiss from discrete chorus emissions. *Nature*, *452*(7183), 62–66. https://doi.org/10.1038/nature06741

Breneman, A. W., Kletzing, C. A., Pickett, J., Chum, J., & Santolik, O. (2009). Statistics of multispacecraft observations of chorus dispersion and source location. *Journal of Geophysical Research*, *114*(A6), A05215. https://doi.org/10.1029/2008JA013549

Burtis, W. J., & Helliwell, R. A. (1969). Banded chorus—A new type of VLF radiation observed in the magnetosphere by OGO 1 and OGO 3. *Journal of Geophysical Research*, *74*(11), 3002–3010. https://doi.org/10.1029/JA074i011p03002

Chan, K.-W., & Holzer, R. E. (1976). ELF hiss associated with plasma density enhancements in the outer magnetosphere. *Journal of Geophysical Research*, *81*(13), 2267–2274. https://doi.org/10.1029/JA081i013p02267

Chen, L., Bortnik, J., Li, W., Thorne, R. M., & Horne, R. B. (2012). Modeling the properties of plasmaspheric hiss: 1. Dependence on chorus wave emission. *Journal of Geophysical Research*, *117*(A5), A05201. https://doi.org/10.1029/2011JA017201

Desai, M., & Giacalone, J. (2016). Large gradual solar energetic particle events. *Living Reviews in Solar Physics*, *13*(1), 3. https://doi.org/10.1007/s41116-016-0002-5

Falkowski, B. J., Tsurutani, B. T., Lakhina, G. S., & Pickett, J. S. (2017). Two sources of dayside intense, quasi-coherent plasmaspheric hiss: A new mechanism for the slot region? *Journal of Geophysical Research: Space Physics*, *122*(2), 1643–1657. https://doi.org/10.1002/2016JA023289

Fukizawa, M., Sakanoi, T., Miyoshi, Y., Hosokawa, K., Shiokawa, K., Katoh, Y., et al. (2018). Electrostatic electron cyclotron harmonic waves as a candidate to cause pulsating auroras. *Geophysical Research Letters*, *45*(23), 12661–12668. https://doi.org/10.1029/2018GL080145

Gatsonis, S.-L. T. N. M. E. G. C. A., Glickman, M. E., & Gatsonis, C. A. (1997). Statistical methods for profiling providers of medical care: Issues and applications. *Journal of the American Statistical Association*, *92*(439), 803–814. https://doi.org/10.1080/01621459.1997.10474036

Gopalswamy, N., Yashiro, S., Krucker, S., Stenborg, G., & Howard, R. A. (2004). Intensity variation of large solar energetic particle events associated with coronal mass ejections. *Journal of Geophysical Research*, *109*(A12), A12105. https://doi.org/10.1029/2004JA010602

Hartley, D. P., Kletzing, C. A., Santolík, O., Chen, L., & Horne, R. B. (2018). Statistical properties of plasmaspheric hiss from Van Allen probes observations. *Journal of Geophysical Research: Space Physics*, *123*(4), 2605–2619. https://doi.org/10.1002/2017JA024593

Hayakawa, M., Ohmi, N., Parrot, M., & Lefeuvre, F. (1986). Direction finding of ELF hiss emissions in a detached plasma region of the magnetosphere. *Journal of Geophysical Research*, *91*(A1), 135–142. https://doi.org/10.1029/JA091iA01p00135

Horne, R. B., Thorne, R. M., Meredith, N. P., & Anderson, R. R. (2003). Diffuse auroral electron scattering by electron cyclotron harmonic and whistler mode waves during an isolated substorm. *Journal of Geophysical Research*, *108*(A7), 1290. https://doi.org/10.1029/2002JA009736

Kataoka, R., Nakagawa, Y., & Sato, T. (2015). Radiation dose of aircrews during a solar proton event without ground-level enhancement. *Annales Geophysicae*, *33*(1), 75–78. https://doi.org/10.5194/angeo-33-75-2015

Kennel, C. F., Scarf, F. L., Fredricks, R. W., McGehee, J. H., & Coroniti, F. V. (1970). Vlf electric field observations in the magnetosphere. *Journal of Geophysical Research*, *75*(31), 6136–6152. https://doi.org/10.1029/JA075i031p06136

Kennel, C. F., & Petschek, H. E. (1966). Limit on stably trapped particle fluxes. *Journal of Geophysical Research*, *71*, 1–28. https://doi.org/10.1029/jz071i001p00001

Kletzing, C. A., Kurth, W. S., Acuna, M., MacDowall, R. J., Torbert, R. B., Averkamp, T., et al. (2013). The electric and magnetic field instrument suite and integrated science (EMFISIS) on RBSP. *Space Science Reviews*, *179*(1–4), 127–181. https://doi.org/10.1007/s11214-013-9993-6

Knipp, D. J. (2017). Essential science for understanding risks from radiation for airline passengers and crews. *Space Weather*, *15*(4), 549–552. https://doi.org/10.1002/2017SW001639

Kurita, S., Miyoshi, Y., Cully, C. M., Angelopoulos, V., Contel, O. L., Hikishima, M., & Misawa, H. (2014). Observational evidence of electron pitch angle scattering driven by ECH waves. *Geophysical Research Letters*, *41*(22), 8076–8080. https://doi.org/10.1002/2014GL061927

Lauben, D. S., Inan, U. S., Bell, T. F., & Gurnett, D. A. (2002). Source characteristics of ELF/VLF chorus. *Journal of Geophysical Research (Space Physics)*, *107*(A12), 1429. https://doi.org/10.1029/2000JA003019

LeDocq, M. J., Gurnett, D. A., & Hospodarsky, G. B. (1998). Chorus source locations from VLF poynting flux measurements with the polar spacecraft. *Geophysical Research Letters*, *25*(21), 4063–4066. https://doi.org/10.1029/1998GL900071

Lyons, L. R., & Thorne, R. M. (1973). Equilibrium structure of radiation belt electrons. *Journal of Geophysical Research*, *78*(13), 2142–2149. https://doi.org/10.1029/JA078i013p02142

Lyons, L. R., Thorne, R. M., & Kennel, C. F. (1972). Pitch-angle diffusion of radiation belt electrons within the plasmasphere. *Journal of Geophysical Research*, *77*(19), 3455–3474. https://doi.org/10.1029/JA077i019p03455

Malaspina, D. M., Ripoll, J.-F., Chu, X., Hospodarsky, G., & Wygant, J. (2018). Variation in plasmaspheric hiss wave power with plasma density. *Geophysical Research Letters*, *45*(18), 9417–9426. https://doi.org/10.1029/2018GL078564

Mauk, B. H., Fox, N. J., Kanekal, S. G., Kessel, R. L., Sibeck, D. G., & Ukhorskiy, A. (2013). Science objectives and rationale for the radiation belt storm probes mission. *Space Science Reviews*, *179*(1–4), 3–27. https://doi.org/10.1007/s11214-012-9908-y

Meredith, N. P., Horne, R. B., & Anderson, R. R. (2001). Substorm dependence of chorus amplitudes: Implications for the acceleration of electrons to relativistic energies. *Journal of Geophysical Research*, *106*(A7), 13165–13178. https://doi.org/10.1029/2000JA900156

Meredith, N. P., Horne, R. B., Bortnik, J., Thorne, R. M., Chen, L., Li, W., & Sicard-Piet, A. (2013). Global statistical evidence for chorus as the embryonic source of plasmaspheric hiss. *Geophysical Research Letters*, *40*(12), 2891–2896. https://doi.org/10.1002/grl.50593

Meredith, N. P., Horne, R. B., Glauert, S. A., & Anderson, R. R. (2007). Slot region electron loss timescales due to plasmaspheric hiss and lightning-generated whistlers. *Journal of Geophysical Research (Space Physics)*, *112*(A8), A08214. https://doi.org/10.1029/2007JA012413

Meredith, N. P., Horne, R. B., Sicard-Piet, A., Boscher, D., Yearby, K. H., Li, W., & Thorne, R. M. (2012). Global model of lower band and upper band chorus from multiple satellite observations. *Journal of Geophysical Research (Space Physics)*, *117*(A16), 10225. https://doi.org/10.1029/2012JA017978

Meredith, N. P., Horne, R. B., Thorne, R. M., Summers, D., & Anderson, R. R. (2004). Substorm dependence of plasmaspheric hiss. *Journal of Geophysical Research (Space Physics)*, *109*, 6209. https://doi.org/10.1029/2004JA010387

Mertens, C. J., Meier, M. M., Brown, S., Norman, R. B., & Xu, X. (2013). Nairas aircraft radiation model development, dose climatology, and initial validation. *Space Weather*, *11*(10), 603–635. https://doi.org/10.1002/swe.20100

Min, K., Lee, J., Keika, K., & Li, W. (2012). Global distribution of emic waves derived from themis observations. *Journal of Geophysical Research*, *117*(A5), A05219. https://doi.org/10.1029/2012JA017515

Ni, B., Thorne, R. M., Shprits, Y. Y., & Bortnik, J. (2008). Resonant scattering of plasma sheet electrons by whistler-mode chorus: Contribution to diffuse auroral precipitation. *Geophysical Research Letters*, *35*(11), 11106. https://doi.org/10.1029/2008GL034032

Nishimura, Y., Bortnik, J., Li, W., Thorne, R. M., Chen, L., Lyons, L. R., et al. (2011). Multievent study of the correlation between pulsating aurora and whistler mode chorus emissions. *Journal of Geophysical Research (Space Physics)*, *116*(A15), A11221. https://doi.org/10.1029/2011JA016876

Nishimura, Y., Bortnik, J., Li, W., Thorne, R. M., Lyons, L. R., Angelopoulos, V., et al. (2010). Identifying the driver of pulsating aurora. *Science*, *330*(6000), 81–84. https://doi.org/10.1126/science.1193186

Olsen, M., Rosey, E., & Tomich, C.-S. (1993). Isolation and analysis of novel mutants of Escherichia coli prlA (secY). *Journal of Bacteriology*, *175*(21), 7092–7096. https://doi.org/10.1128/jb.175.21.7092-7096.1993

Parrot, M., & Lefeuvre, F. (1986). Statistical study of the propagation characteristics of ELF hiss observed on GEOS-1, inside and outside the plasmasphere. *Annales Geophysicae*, *4*, 363–383.

Reames, D. (2013). The two sources of solar energetic particles. *Space Science Reviews*, *175*(1–4), 53–92. https://doi.org/10.1007/s11214-013-9958-9

Saikin, A. A., Zhang, J.-C., Allen, R. C., Smith, C. W., Kistler, L. M., Spence, H. E., et al. (2015). The occurrence and wave properties of H+-He+-and O+-band EMIC waves observed by the Van Allen probes. *Journal of Geophysical Research: Space Physics*, *120*(9), 7477–7492. https://doi.org/10.1002/2015JA021358

Sheeley, B. W., Moldwin, M. B., Rassoul, H. K., & Anderson, R. R. (2001). An empirical plasmasphere and trough density model: CRRES observations. *Journal of Geophysical Research*, *106*(A11), 25631–25642. https://doi.org/10.1029/2000JA000286

Summers, D., Ni, B., & Meredith, N. P. (2007). Timescales for radiation belt electron acceleration and loss due to resonant wave-particle interactions: 2. Evaluation for VLF chorus, ELF hiss, and electromagnetic ion cyclotron waves. *Journal of Geophysical Research (Space Physics)*, *112*(A4), 4207. https://doi.org/10.1029/2006JA011993

Thorne, R. M. (2010). Radiation belt dynamics: The importance of wave-particle interactions. *Geophysical Research Letters*, *37*(22), 22107. https://doi.org/10.1029/2010GL044990

Thorne, R. M., Smith, E. J., Burton, R. K., & Holzer, R. E. (1973). Plasmaspheric hiss. *Journal of Geophysical Research*, *78*(10), 1581–1596. https://doi.org/10.1029/JA078i010p01581

Tobiska, W. K., Bouwer, D., Smart, D., Shea, M., Bailey, J., Didkovsky, L., et al. (2016). Global real-time dose measurements using the automated radiation measurements for aerospace safety (ARMAS) system. *Space Weather*, *14*(11), 1053–1080. https://doi.org/10.1002/2016SW001419

Tobiska, W. K., Didkovsky, L., Judge, K., Weiman, S., Bouwer, D., Bailey, J., et al. (2018). Analytical representations for characterizing the global aviation radiation environment based on model and measurement databases. *Space Weather*, *16*(10), 1523–1538. https://doi.org/10.1029/2018SW001843

Tobiska, W. K., Halford, A. J., & Morley, S. K. (2022). Increased radiation events discovered at commercial aviation altitudes. *Space Weather*. https://doi.org/10.48550/arXiv.2209.05599

Tsurutani, B. T., Falkowski, B. J., Pickett, J. S., Santolik, O., & Lakhina, G. S. (2015). Plasmaspheric hiss properties: Observations from polar. *Journal of Geophysical Research: Space Physics*, *120*(1), 414–431. https://doi.org/10.1002/2014JA020518

Tsurutani, B. T., Hajra, R., Tanimori, T., Takada, A., Remya, B., Mannucci, A. J., et al. (2016). Heliospheric plasma sheet (HPS) impingement onto the magnetosphere as a cause of relativistic electron dropouts (REDs) via coherent emic wave scattering with possible consequences for climate change mechanisms. *Journal of Geophysical Research: Space Physics*, *121*(10), 10130–10156. https://doi.org/10.1002/2016JA022499

Tsurutani, B. T., Park, S. A., Falkowski, B. J., Lakhina, G. S., Pickett, J. S., Bortnik, J., et al. (2018). Plasmaspheric hiss: Coherent and intense. *Journal of Geophysical Research: Space Physics*, *123*(12), 10009–10029. https://doi.org/10.1029/2018JA025975

Tsurutani, B. T., & Smith, E. J. (1974). Postmidnight chorus: A substorm phenomenon. *Journal of Geophysical Research*, *79*(1), 118–127. https://doi.org/10.1029/JA079i001p00118

Usanova, M. E., Mann, I. R., Bortnik, J., Shao, L., & Angelopoulos, V. (2012). Themis observations of electromagnetic ion cyclotron wave occurrence: Dependence on ae, symh, and solar wind dynamic pressure. *Journal of Geophysical Research*, *117*(A10), A10218. https://doi.org/10.1029/2012JA018049

Vlahos, L., Anastasiadis, A., Papaioannou, A., Kouloumvakos, A., & Isliker, H. (2019). Sources of solar energetic particles. *Philosophical Transactions of the Royal Society A: Mathematical, Physical & Engineering Sciences*, *377*(2148), 20180095. https://doi.org/10.1098/rsta.2018.0095

Wygant, J. R., Bonnell, J. W., Goetz, K., Ergun, R. E., Mozer, F. S., Bale, S. D., et al. (2013). The electric field and waves instruments on the radiation belt storm probes mission. *Space Science Reviews*, *179*(1–4), 183–220. https://doi.org/10.1007/s11214-013-0013-7

Yu, X., Yuan, Z., & Ouyang, Z. (2021). First observations of O2+ band emic waves in the terrestrial magnetosphere. *Geophysical Research Letters*, *48*(19), e2021GL094681. https://doi.org/10.1029/2021GL094681

Yu, X., Yuan, Z., Wang, D., Li, H., Huang, S., Wang, Z., et al. (2015). In situ observations of emic waves in O+ band by the Van Allen Probe A. *Geophysical Research Letters*, *42*(5), 1312–1317. https://doi.org/10.1002/2015GL063250

Zhang, S., Rae, I. J., Watt, C. E. J., Degeling, A. W., Tian, A., Shi, Q., et al. (2021). Determining the temporal and spatial coherence of plasmaspheric hiss waves in the magnetosphere. *Journal of Geophysical Research: Space Physics*, *126*(2), e2020JA028635. https://doi.org/10.1029/2020JA028635